LRRC3B, Encoding a Leucine-Rich Repeat-Containing Protein, Is a Putative Tumor Suppressor Gene in Gastric Cancer

Mirang Kim,[1,7] Jeong-Hwan Kim,[1] Hay-Ran Jang,[1] Hwan-Mook Kim,[2] Chang-Woo Lee,[2] Seung-Moo Noh,[3] Kyu-Sang Song,[4] June-Sik Cho,[5] Hyun-Yong Jeong,[6] Yoonsoo Hahn,[8] Young-Il Yeom,[1] Hyang-Sook Yoo,[1] and Yong Sung Kim[1,7]

[1]Medical Genomics Research Center, [2]Bio-Evaluation Center, Korea Research Institute of Bioscience and Biotechnology, Departments of [3]General Surgery, [4]Pathology, [5]Diagnostic Radiology, and [6]Internal Medicine, College of Medicine, Chungnam National University, and [7]Department of Functional Genomics, University of Science & Technology, Daejeon, Korea; and [8]Department of Life Science, Chung-Ang University, Seoul, Korea

Abstract

Leucine-rich repeat-containing 3B (LRRC3B) is an evolutionarily highly conserved leucine-rich repeat-containing protein, but its biological significance is unknown. Using restriction landmark genomic scanning and pyrosequencing, we found that the promoter region of *LRRC3B* was aberrantly methylated in gastric cancer. Gastric cancer cell lines displayed epigenetic silencing of *LRRC3B*, but treatment with the DNA methylation inhibitor 5-aza-2′-deoxycytidine and/or the histone deacetylase inhibitor trichostatin A increased *LRRC3B* expression in gastric cancer cell lines. Real-time reverse transcription-PCR analysis of 96 paired primary gastric tumors and normal adjacent tissues showed that *LRRC3B* expression was reduced in 88.5% of gastric tumors compared with normal adjacent tissues. Pyrosequencing analysis of the promoter region revealed that *LRRC3B* was significantly hypermethylated in gastric tumors. Stable transfection of *LRRC3B* in SNU-601 cells, a gastric cancer cell line, inhibited anchorage-dependent and anchorage-independent colony formation, and *LRRC3B* expression suppressed tumorigenesis in nude mice. Microarray analysis of *LRRC3B*-expressing xenograft tumors showed induction of immune response–related genes and IFN signaling genes. H&E-stained sections of *LRRC3B*-expressing xenograft tumors showed lymphocyte infiltration in the region. We suggest that *LRRC3B* is a putative tumor suppressor gene that is silenced in gastric cancers by epigenetic mechanisms and that *LRRC3B* silencing in cancer may play an important role in tumor escape from immune surveillance. [Cancer Res 2008;68(17):7147–55]

Introduction

Leucine-rich repeat (LRR)-containing 3B (LRRC3B) is a putative LRR-containing transmembrane protein found by the Secreted Protein Discovery Initiative undertaken to identify new secreted and transmembrane proteins (1). LRRs are protein interaction motifs of 20 to 29 amino acid residues characterized by repetition of hydrophobic residues, especially leucine, and that are separated by conserved distance (2–4). LRR-containing proteins, of which there are >2,000, participate in many important processes, including plant and animal immunity, hormone-receptor interactions, cell adhesion, signal transduction, regulation of gene expression, and apoptosis (5, 6). A number of microarray expression profiling studies on human cancers have shown that *LRRC3B* is down-regulated in gastric (7), breast (8), colon (9), testis (10), prostate (11), and brain cancers (12), suggesting *LRRC3B* involvement in carcinogenesis.

DNA methylation associated with histone modification is a key mechanism to inhibit the expression of tumor suppressor genes in cancer, and DNA methylation markers have been applied in cancer risk assessment, early detection, prognosis, and prediction of response to cancer therapy (13–15). We have used restriction landmark genomic scanning (RLGS) to identify methylation markers in gastric cancer on a whole-genome scale (16). We previously reported aberrant methylation of *LIMS2*, a regulator of cell migration (17), *DCBLD2*, a cell growth repressor (18), and *Protein kinase D1* (19) in gastric cancer by RLGS and pyrosequencing, a quantitative methylation analysis of multiple CpG sites.

Here, we report the identification of *LRRC3B* as a target of aberrant methylation in gastric cancer and show *LRRC3B* silencing by epigenetic mechanisms in gastric cancer cell lines and primary gastric tumor tissues. We also examined the function of *LRRC3B* as a tumor suppressor *in vitro* and *in vivo* and provide evidence that loss of *LRRC3B* function in gastric cancer likely promotes tumor escape from immune surveillance.

Materials and Methods

Cell lines and tissue samples. Ninety-six pairs of frozen gastric tumors and normal adjacent tissues were accessed from the Stomach Cancer Bank at Chungnam National University Hospital, Daejeon, Korea, as described (17–19). Specimens were originally obtained from tumors immediately after resection. Corresponding normal mucosa specimens were at least 3 cm away from the tumor edge. All samples were obtained with informed consent, and their use was approved by the Institutional Review Board of the Chungnam National University Hospital, Daejeon, Korea. Gastric cancer cell lines established from gastric cancer patients (20, 21) were obtained from the Korean Cell Line Bank[9] and were cultured in RPMI 1640 supplemented with 10% fetal bovine serum (FBS) and 1% antibiotic-antimycotic solution (Invitrogen).

RLGS, spot cloning, and sequence analysis. RLGS was performed as described (16, 22, 23). DNA fragments corresponding to a spot of interest on

Note: Supplementary data for this article are available at Cancer Research Online (http://cancerres.aacrjournals.org/).

M. Kim and J.-H. Kim contributed equally to this work.

Requests for reprints: Yong Sung Kim, Medical Genomics Research Center, Korea Research Institute of Bioscience and Biotechnology, 52 Eoeun-dong, Yuseong-gu, Daejeon 305-806, Korea. Phone: 82-42-879-8110; Fax: 82-42-879-8119; E-mail: yongsung@kribb.re.kr.

doi:10.1158/0008-5472.CAN-08-0667

[9] http://cellbank.snu.ac.kr

two-dimensional gels were cloned as described (24). Briefly, 10 μg DNA from normal tissue was digested sequentially with *Not*I and *Eco*RV, and directly mixed with 2 μg labeled DNA for the first dimensional separation. This mixture was then subjected to RLGS. After the second-dimension separation, the gel was covered with plastic wrap and affixed to an imaging plate without drying. The overnight-exposed imaging plate was scanned using the BAS3000 system (FUJI Photo Film Co.) and printed on a transparent film. The film was overlaid on the original gel, and the portion of the gel corresponding to the spot was cut out and the DNA was purified. After DNA ligation with biotinylated *Not*I and *Hin*fI linkers (24), iron-coated streptavidin (Dynabeads M280 streptavidin; Dynal, Inc.) was added, and the DNAs trapped with the linkers were recovered and washed. A high-salt buffer was used to wash the beads, and the purified DNA was then amplified for 30 PCR cycles using 200 nmol/L each of primers I and primer II (24). The amplified DNA fragment was cloned into the *Sma*I site of plasmid pUC19.

Southern blot hybridization analysis. Genomic DNA from paired normal and tumor tissue and lymph node tissue from one patient and from SNU-005 gastric cancer cell line was digested with *Not*I/*Eco*RV, *Not*I/*Hin*fI, or *Hin*fI alone (New England Biolabs) for 4 h. The digested DNAs were separated on a 0.8% agarose gel, transferred to a nylon membrane (Amersham Biosciences), and hybridized with a DNA probe (25). The probe was prepared by purifying *Hin*fI/*Not*I-digested fragments from the plasmid containing the DNA that generated spot 3C43 and randomly priming the fragments with [α-^{32}P]dATP with Prime-It II kit (Stratagene).

Promoter reporter assay. A 702-bp fragment of *LRRC3B* (−238 to +462 with respect to the transcription start site) was obtained by PCR using the forward primer 5′-CGAGAGCAGCAGAGGGAGT-3′ and the reverse primer 5′-GCTCTGCGAAAAGCAACAG-3′ and inserted into the pGEM-T Easy vector (Promega). Then, the *Nco*I/*Sac*I fragment was inserted into the pGL3-Basic vector (Promega) that contains a modified firefly luciferase gene to make pLRRC3BCpG71-luc. pRL-CMV vector (Promega) was used to normalize the transfection efficiency. DNA (0.8 μg pLRRC3BCpG71-luc DNA and 0.2 μg pRL-CMV DNA) was transfected into SNU-484 cells using Lipofectamine Plus reagent (Invitrogen) according to the manufacturer's protocol. The pGL3-Basic vector was used as a negative control. Firefly and *Renilla* luciferase activities were measured 48 h after transfection. Relative luciferase activities were calculated after normalization of the transfection efficiency by *Renilla* luciferase activity.

Real-time reverse transcription-PCR analysis. Real-time reverse transcription-PCR (RT-PCR) was performed as described (17–19). Total cellular RNA (5 μg) was reverse transcribed into cDNA using SuperScript II (Invitrogen). Real-time PCR was preformed using the Exicycler Quantitative Thermal Block (BiONEER). The RT reaction product (100 ng) was amplified in a 15-μL reaction volume with 2× SYBR Premix EX Taq (Takara). We used the Primer3 program[10] to design the *LRRC3B* exon 2 forward (5′-TTCCCTCTCCATGTGTCTCC-3′) and reverse (5′-CCAGCATGTTCATCCAA-CAC-3′) primers. Samples were heated to 95°C for 1 min and then amplified for 45 cycles consisting of 95°C for 30 s, 60°C for 30 s, and 72°C for 30 s, followed by a final extension step of 72°C for 10 min. *β-actin* was used as an internal control. Relative quantification of *LRRC3B* mRNA was analyzed by the comparative threshold cycle (C_T) method (26).

Bisulfite sequencing. Genomic DNA (1 μg) was modified by sodium bisulfite using the EZ DNA Methylation kit (ZYMO Research) according to the manufacturer's instructions. For amplification of bisulfite-modified DNA, we used the MethPrimer program[11] to design the forward primer 5′-TATTTTTAGTTTGGGTTTGG-3′ and reverse primer 5′-TAATTCTCCTC-TACTTATTCCTTAA-3′ to yield a 555-bp product size. Bisulfite-modified DNA (1 μL) was amplified in a 20-μL volume containing primers. Samples were heated to 95°C for 12 min and then amplified for 35 cycles consisting of 95°C for 45 s, 50°C for 45 s, and 72°C for 60 s, then incubated at 72°C for 10 min and cooled to 4°C. The PCR products were visualized on a 1% agarose gel by ethidium bromide staining, purified from the gel using the Qiagen Gel Extraction kit, and cloned using the pGEM-T Easy Vector (Promega). Ten clones were randomly chosen for sequencing. Complete bisulfite conversion was assured when <0.01% of the cytosines in non-CG dinucleotides in the final sequence had not converted.

5-Aza-2′-deoxycytidine and trichostatin A treatment. SNU-216, SNU-601, and SNU-638 cell lines were seeded at a density of 1×10^6 cells per 10-cm dish and cultured for 1 d before drug treatment. The cells were treated with 1 μmol/L 5-aza-2′-deoxycytidine (5-aza-dC; Sigma) every 24 h for 3 d and then harvested. Another culture of cells was treated with 250 nmol/L trichostatin A (TSA; Sigma) for 1 d and then harvested. To test the synergistic effects of 5-aza-dC and TSA, the cells were first treated with 1 μmol/L 5-aza-dC for 3 d, followed by treatment with 250 nmol/L TSA for 1 d. Total RNA was prepared, and the effect on *LRRC3B* expression was assessed by real-time RT-PCR.

Chromatin immunoprecipitation assay. A chromatin immunoprecipitation (ChIP) assay was performed with a ChIP assay kit (Upstate Biotechnology) according to the manufacturer's protocol with modifications (19). Briefly, proteins were crosslinked to DNA by addition of formaldehyde directly to the culture medium to a final concentration of 1% for 10 min at 37°C. The collected cells were washed twice with ice-cold PBS with proteinase inhibitors and resuspended in 200 μL SDS lysis buffer (Upstate Biotechnology) per 1×10^6 cells. Lysates were sonicated 21 times for 5 s with 30-s intervals on ice, at power setting 3 (Fisher Sonicator Dismembrator 100). These shearing conditions yielded DNA fragments ranging from 200 to 500 bp. The sheared samples were centrifuged at 12,000 × *g* for 10 min at 4°C, and the supernatants were diluted in 9 volumes of ChIP dilution buffer (Upstate Biotechnology). The cell supernatants were precleared with salmon sperm DNA/protein A agarose beads (Upstate Biotechnology) then immunoprecipitated with 5 μL of antibody to either acetyl-histone H3 (Upstate Biotechnology) or acetyl-histone H4 (Upstate Biotechnology), or no antibody. Immunoprecipitated DNA was recovered using the QIAquick PCR Purification kit (Qiagen) and analyzed by real-time PCR using the primers 5′-GTCACGTTAATTCCC-TGCTG-3′ and 5′-TTGCAGGAAGAGCAGACAAA-3′ (located in the *LRRC3B* CpG island; Fig. 1*A*). Samples were heated to 95°C for 1 min and then amplified for 45 cycles of 95°C for 30 s, 58°C for 30 s, and 72°C for 30 s. The amount of immunoprecipitated DNA was normalized to the input DNA.

Pyrosequencing. The promoter region of *LRRC3B* was PCR amplified using forward primer 5′-GAGGTATTGGTTGGGTTTTG-3′ and biotinylated reverse primer 5′-AACCCAACTACCCACCTAA-3′ designed by PSQ Assay Design (Biotage AB). The product size was 420 bp. Bisulfite-modified DNA (3 μL) was amplified in a 25-μL volume with the primers and 2× Premix EX Taq (Takara). Samples were heated to 95°C for 5 min and then amplified for 50 cycles of 95°C for 30 s, 60°C for 40 s, and 72°C for 30 s, followed by a final extension step at 72°C for 5 min. Pyrosequencing reactions were performed according to the manufacturer's specifications with a sequencing primer 5′-GTTTGG AGTAGGGTTTGTAG-3′ and run on the PSQ HS 96A System (Biotage AB). Six CpG sites were analyzed. The expected sequence was YGGTYGTYGTAGTAAYGYGAGTTAAGTYG (Y = T or C).

Transfection and colony formation assay. Because the *LRRC3B* coding region lies entirely within exon 2, the entire *LRRC3B* coding sequence was amplified from human genomic DNA by PCR using the primers *Bam*HI_LRRC3B_F 5′-GGATCCATGAATCTGGTAGACCTG-3′ and *Xho*I_LRRC3B_R 5′-CTCGAGCTATACCACAGTGCTAAT-3′ and cloned into the pGEM-T Easy vector. After confirming the sequences, the full-length *LRRC3B* cDNA was subcloned into pcDNA3.1 (Invitrogen) at the *Bam*HI and *Xho*I sites. For a colony formation assay in a monolayer culture, SNU-601 cells were plated at 3×10^5 cells per well in 6-well plates, and transfected with either pcDNA3.1-LRRC3B or empty vector control pcDNA3.1 using Lipofectamine Plus reagent. The cells were selected with G418 (500 μg/mL) for 4 wk. Two positive clones and one control clone were plated in 6-well plates at 200 or 400 cells per well. After 2 wk of incubation with G418, the cells were stained with crystal violet. To study colony formation in soft agar, the stable transfectants were suspended in RPMI 1640 containing 0.3% agarose, 10% FBS, and 500 μg/mL G418 and layered on RPMI 1640

[10] http://frodo.wi.mit.edu/cgi-bin/primer3/primer3_www.cgi
[11] http://www.urogene.org/methprimer/index.html

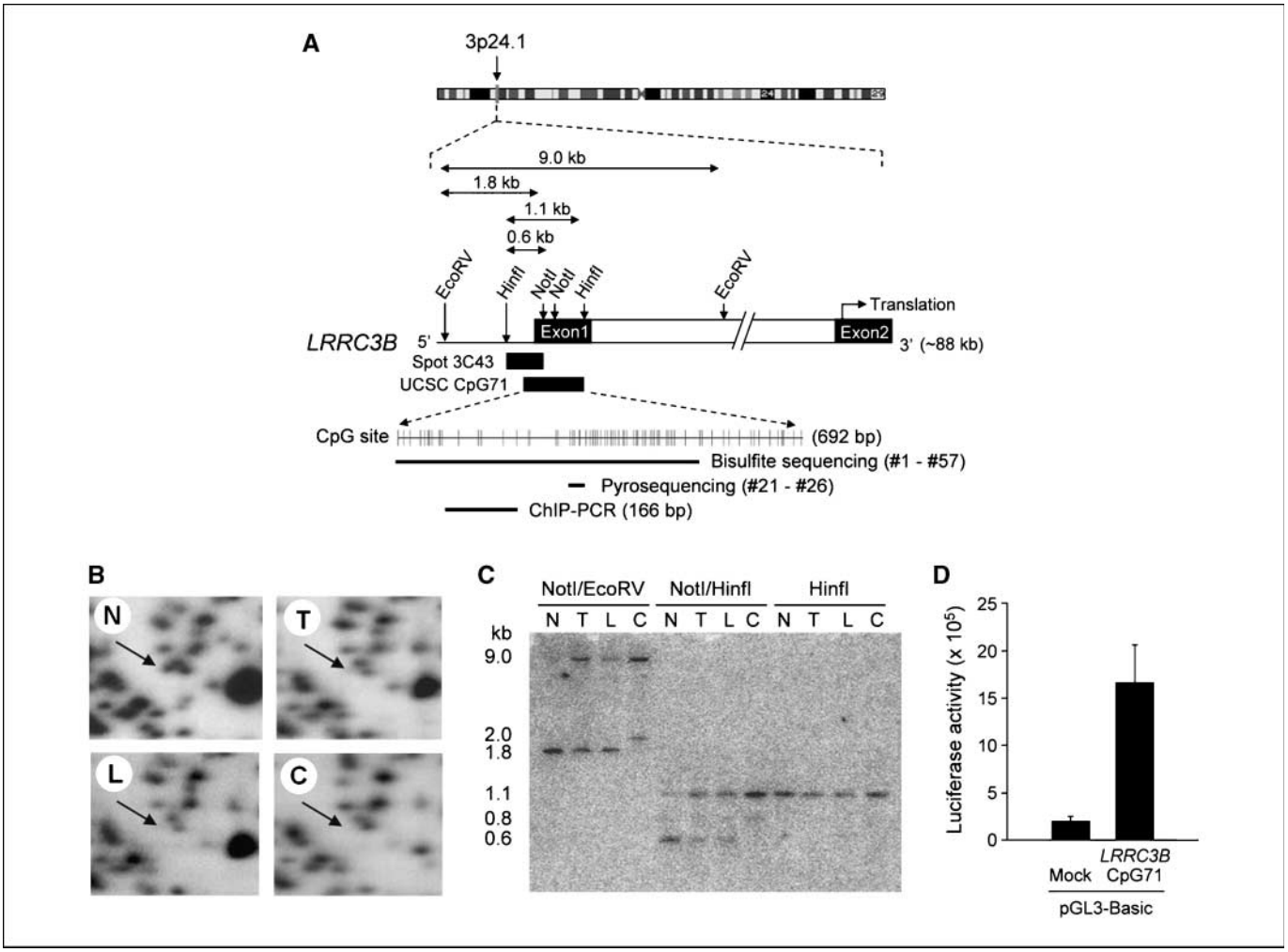

Figure 1. RLGS analysis and schematic structure of *LRRC3B. A, LRRC3B* structure and restriction enzyme map. *LRRC3B*, which contains two exons, covers about 88 kb at the human chromosome 3p24.1 locus. The sequence of the RLGS spot 3C43 (*Not*I/*Hin*fI fragment) was identical to the 5′ upstream region and exon 1 of *LRRC3B* and overlaped with CpG island 71 predicted by the UCSC genome server, May 2004 Freeze.[12] The expected fragment sizes resulting from digestion with *Not*I/*Hin*fI, *Hin*fI/*Hin*fI, *Not*I/*Eco*RV, and *Eco*RV/*Eco*RV were 625 bp (0.6 kb), 1,137 bp (1.1 kb), 1,844 bp (1.8 kb), and 8,976 bp (9.0 kb), respectively, as shown. Among the 71 CpG sites of CpG island 71, CpG numbers 1 to 57 were subjected to bisulfite sequencing, and CpG numbers 21 to 26 were subjected to pyrosequencing. Location of the DNA fragments amplified by ChIP-PCR is shown. *B,* comparison of the 3C43 spot intensity in a section of the RLGS gel. *Arrows,* 3C43 spots in normal mucosa (*N*), primary tumor (*T*), and lymph node (*L*) from one patient and the gastric cancer cell line SNU-005 (*C*). *C,* Southern blot hybridization using the 3C43 spot DNA as a probe. Genomic DNAs from normal mucosa, primary tumor, and lymph node tissues from one patient, and from SNU-005, were digested with *Not*I and *Eco*RV, *Not*I and *Hin*fI, or *Hin*fI alone. *D,* promoter activity of the *LRRC3B* CpG island. pGL3-Basic empty vector (*mock*) and the vector containing the *LRRC3B* CpG island (−238 to +462) were transfected into SNU-484 cells. Luciferase activity was normalized to an internal control. *Columns,* mean from four independent experiments; *bars,* SD.

containing 0.6% agarose, 10% FBS, and G418 in a 6-well plate. Colonies were photographed and counted after 2 wk of incubation at 37°C.

Subcellular localization of LRRC3B. To study LRRC3B subcellular localization, the entire *LRRC3B* coding sequence (without a stop codon) was amplified from human genomic DNA by PCR using the primers *Hin*dIII_LRRC3B_F 5′-CAAGCTTCGATGAATCTGGTAGACCTG-3′ and *Bam*HI_LRRC3B_R 5′-GGATCCTACCACAGTGCTAATATC-3′, and cloned into the pGEM-T Easy vector. After confirming the sequences, the full-length *LRRC3B* cDNA was subcloned into pEGFP-N3 (Clontech) at the *Hin*dIII and *Bam*HI sites to generate a COOH-terminal green fluorescent protein (GFP) fusion protein. SNU-601 cells were seeded on 25-mm diameter coverslips. pEGFP-N3-LRRC3B or control vector was transfected into the cells using Lipofectamine Plus. At 2 d posttransfection, the cells were observed under a Zeiss LSM 510 confocal laser scanning microscope (Zeiss).

Tumorigenesis assay in nude mice. We maintained 3-wk-old male nude mice (Japan SLC, Inc.) in accordance with the guidelines and under approval of the Institutional Review Committee for the Animal Care and Use, Korea Research Institute of Bioscience and Biotechnology. Two clones of SNU-601 cells stably expressing *LRRC3B* and vector control–transfected cells were used in a tumorigenesis assay. For the tumorigenesis assay, cells were collected by centrifugation, washed twice in PBS, and 3×10^6 cells were resuspended in 0.1 mL of PBS and injected s.c. into nude mice (7 mice per cell line). We measured tumor volume as described (27).

Microarray analysis. Microarray analysis was performed as described (28). Briefly, total cellular RNA (20 μg) from xenograft tumors and SNU-601 cells was used as template for the synthesis of Cy5- or Cy3-labeled (Genisphere, Inc.) cDNA using SuperScript II reverse transcriptase (Invitrogen) for 2 h at 42°C. The two labeled cDNAs were mixed together, filtered through Microcon YM-30 membrane (Millipore) to exclude unincorporated deoxynucleotide triphosphates, and hybridized to the cDNA microarray slide (containing 23,232 genes and 1,056 controls; Korea Research Institute of Bioscience and Biotechnology) at 50°C overnight using

[12] http://genome.ucsc.edu/

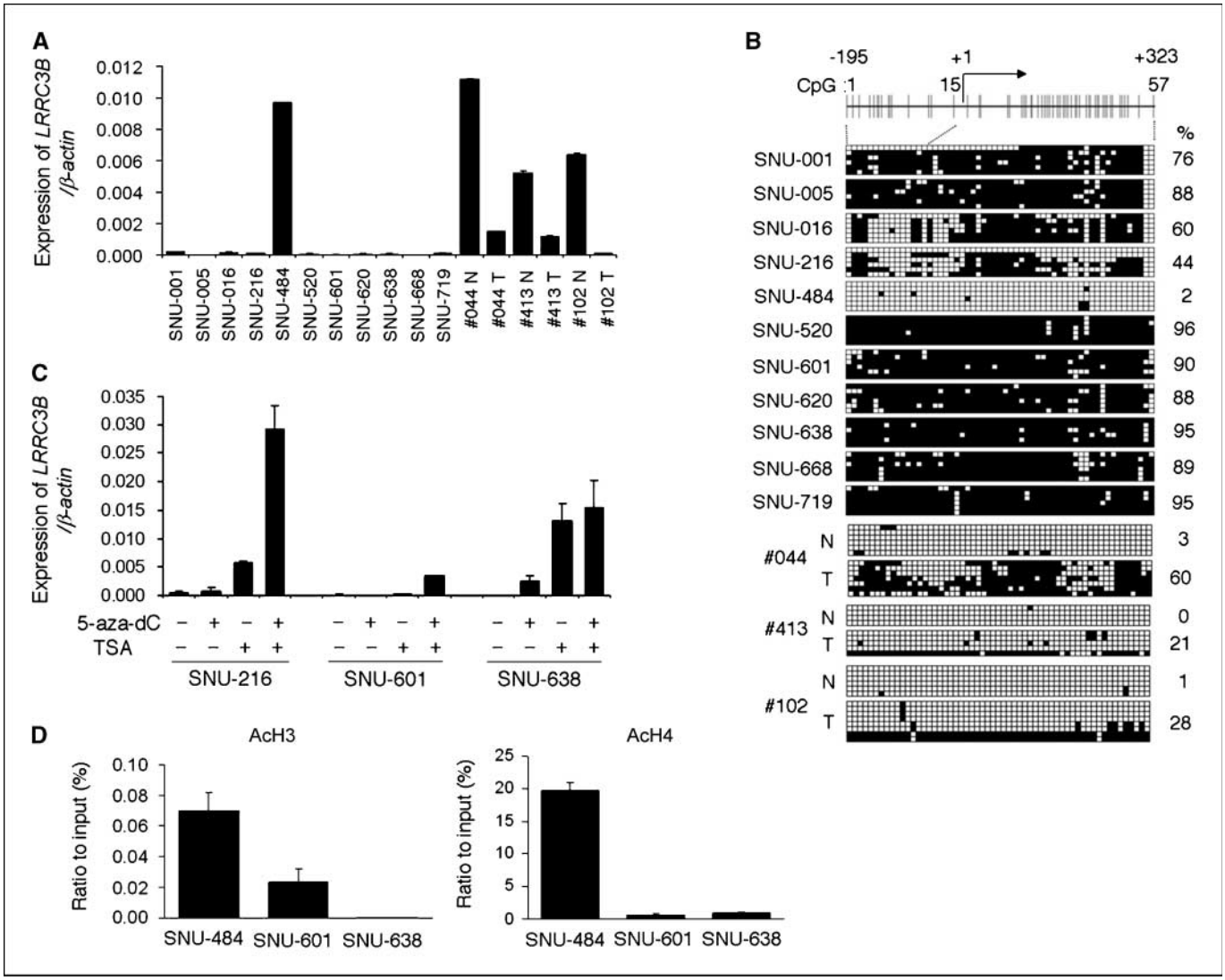

Figure 2. Expression and methylation analysis of *LRRC3B* in gastric cancer cell lines and gastric cancer tissues. *A,* real-time RT-PCR analysis of *LRRC3B* mRNA in 11 gastric cancer cell lines and three pairs of gastric tumor (*T*) and normal (*N*) tissues. *B,* bisulfite sequencing analysis of *LRRC3B* CpG sites in 11 gastric cancer cell lines and three pairs of gastric and normal tissues. The bisulfite sequencing covers 57 CpG sites in the *LRRC3B* CpG island (see Fig. 1*A*). *Open squares,* unmethylated CpG sites; *filled squares,* methylated CpG sites. Each row represents a single clone. The numbers on the right represent the mean percentages of CpG sites that were methylated for each cell line or tissue. *+1,* transcription start site. *C,* restoration of *LRRC3B* expression by treatment with 5-aza-dC and/or TSA in gastric cancer cell lines. SNU-216, SNU-601, and SNU-638 cells were treated with the inhibitors as described in the Materials and Methods. Total RNA was isolated, and *LRRC3B* expression was determined by real-time RT-PCR. *Columns,* mean of three independent experiments; *bars,* SD. *D,* ChIP assays of the *LRRC3B* CpG island. Chromatin DNA was immunoprecipitated with antibodies specific for acetylated histone H3 (*AcH3*) or acetylated histone H4 (*AcH4*). DNA fragments corresponding to the *LRRC3B* CpG island (see Fig. 1*A*) were amplified by PCR. The amount of immunoprecipitated DNA was normalized to the input DNA. *Columns,* mean from two independent ChIP experiments and a total of four independent PCR analyses; *bars,* SD.

a 3DNA Array 50 kit (Genisphere, Inc.). After hybridization, each microarray was washed twice with 2× SSC containing 0.2% SDS at room temperature for 5 min, and finally with 95% ethanol at room temperature for 1 min. The hybridized slide was scanned by a GenePix 4000B Scanner (Axon Instruments, Inc.) and analyzed using the GenePix Pro 4.0 program (Axon Instruments). Genes with significantly different expression levels according to Student's *t* test in xenograft tumors expressing *LRRC3B* compared with control xenograft tumors were selected (29). We deposited the raw data in Gene Expression Omnibus[13] with an accession number GSE4003.

Immunohistochemistry. Immunohistochemical staining was done as described (30). Briefly, paraffin sections of xenograft tumors were dewaxed, rehydrated, and washed thrice with PBS. After treatment with proteinase K for 5 min at 37°C, sections were treated with H_2O_2 for 10 min at room temperature, blocked in PBS containing 0.1% Tween 20 and 1% bovine serum albumin for 20 min, followed by reaction with anti-mouse NK-1.1 (diluted 1:100; BD Biosciences) for 1 h. Sections were incubated sequentially with peroxidase-conjugated secondary antibody and visualized with ChemMate EnVision detection kit (Dako). Sections without primary antibody were used as negative controls.

Statistical analysis. The Student's *t* test was used to establish the statistical significance of differences in *LRRC3B* expression or *LRRC3B* promoter methylation between primary gastric tumors and adjacent normal tissues. The clinicopathologic factors in various groups of patients were compared using the χ^2 test or Student's *t* test. Results with *P* values of <0.05 were considered statistically significant.

[13] http://www.ncbi.nlm.nih.gov/projects/geo

Results

***LRRC3B* is a target of aberrant methylation in gastric cancer.** RLGS assays were performed on gastric cancer cell lines and gastric cancer tissues to look for aberrant methylation of genomic DNA compared with normal gastric mucosal tissue (16). RLGS profiles of the gastric cancer cell lines showed that 82% (9 of 11) lacked a DNA spot named 3C43, and this spot was decreased in 73% (11 of 15) of the primary tumors tested. Figure 1*B* shows a decrease in the 3C43 spot in tumor and metastatic lymph node tissue from one patient and the gastric cancer cell line SNU-005. The DNA of the 3C43 spot was purified from the RLGS gel and was cloned. Sequence analysis of the cloned 3C43 spot DNA identified it as the sequence of a *Not*I/*Hin*fI fragment covering the 5′ upstream region and first exon of *LRRC3B* at chromosome region 3p24.1. The 3C43 spot DNA sequence also partly overlapped with CpG island 71 predicted in the University of California, Santa Cruz (UCSC) genome browser[14] (Fig. 1*A*).

To understand whether the decrease in the 3C43 spot intensity in the RLGS profiles of the gastric cancers was due to *Not*I site methylation or loss of heterozygosity, we performed Southern blot analysis using the 3C43 spot DNA fragment as a probe. We observed 1.1-kb *Hin*fI-digested bands in all tumor-related DNAs, as well as normal mucosal DNA, indicating that the decreased spot intensity was not due to loss of heterozygosity in this region. We also observed increased intensity of a high molecular weight band in the *Not*I/*Eco*RV-digested and *Not*I/*Hin*fI-digested DNA fragments from a gastric tumor, metastatic lymph node, and a gastric cancer cell line, indicating increased methylation at the *Not*I site in gastric cancer (Fig. 1*C*). This result suggested that the loss or decrease of 3C43 spot intensity in gastric cancer was due to hypermethylation.

To test whether the CpG island 71 is important for transcription of *LRRC3B*, we generated a luciferase reporter construct, named pLRRC3BCpG71-luc, containing a fragment of the entire CpG island 71 (−238 to +462). Construct pLRRC3BCpG71-luc displayed 8.6-fold higher luciferase activity than the control plasmid, pGL3-Basic (Fig. 1*D*), suggesting that the CpG island 71 of *LRRC3B* contains a functional promoter.

***LRRC3B* is down-regulated by DNA methylation and histone deacetylation in gastric cancer.** To investigate a potential relationship between promoter methylation and down-regulation of *LRRC3B* expression in gastric cancer, we analyzed *LRRC3B* mRNA expression levels in 11 gastric cancer cell lines established from Korean gastric cancer patients by real-time RT-PCR. Most of the 11 gastric cancer cell lines showed very low levels of *LRRC3B*; only SNU-484 cells displayed a high level of *LRRC3B* mRNA. We also examined the expression level of *LRRC3B* in three paired gastric cancer and adjacent normal tissue samples. Tumor tissues expressed *LRRC3B* at lower levels than each of the respective paired normal tissues (Fig. 2*A*). Bisulfite sequencing analysis of the *LRRC3B* CpG island (−195 to +323, 57 CpG sites) showed that 44% to 96% of the CpG sites were methylated in 10 gastric cancer cell lines, but SNU-484 cells had methylation at only 2% of the CpG sites in the *LRRC3B* CpG island. Gastric tumor tissues were moderately methylated with methylation at 21% to 60% of the sites, whereas paired normal tissues contained only 0% to 3% methylated CpG sites (Fig. 2*B*), indicating that methylation correlated with reduced *LRRC3B* expression in gastric cancer cell lines and gastric cancer tissues.

DNA methylation is usually linked with histone deacetylation (31). To examine whether silencing of *LRRC3B* in gastric cancer cells could be restored by treatment with the DNA methylation inhibitor 5-aza-dC (32) and/or the histone deacetylase inhibitor TSA (33), we treated cell lines SNU-216, SNU-601, and SNU-638 (in which the *LRRC3B* CpG island is hypermethylated and transcriptionally silenced) with 5-aza-dC, TSA, or both. After treatment, we isolated RNA and measured *LRRC3B* expression by real-time RT-PCR (Fig. 2*C*). *LRRC3B* expression was restored in SNU-216 and SNU-638 cells by treatment with 5-aza-dC or TSA alone. TSA was more effective than 5-aza-dC at inducing *LRRC3B* expression in both cell lines, and the combination of 5-aza-dC and TSA resulted in synergistic reactivation of *LRRC3B* in all cell lines treated. These results provide evidence that both DNA methylation and histone deacetylation have a causal role in silencing of *LRRC3B* expression in gastric cancer cells. To examine local histone acetylation in the chromatin associated with the *LRRC3B* CpG island, we performed a ChIP assay in gastric cell lines having different expression levels of *LRRC3B*. The histone-associated DNAs, immunoprecipitated with antibodies against acetylated histone H3 (K9 and K14) or acetylated histone H4 (K5, K8, K12, and K16), were amplified with a primer set specific for the *LRRC3B* CpG

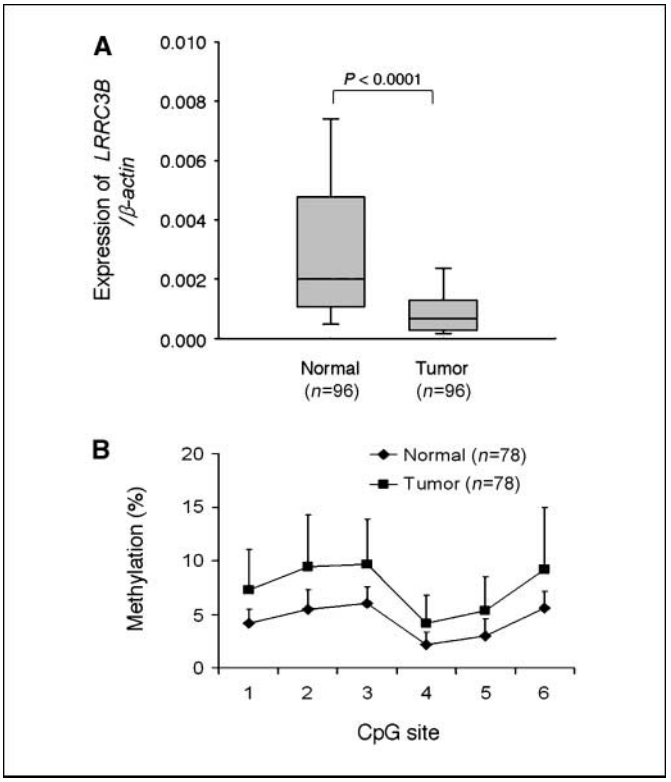

Figure 3. Quantitative evaluation of *LRRC3B* expression and CpG methylation in gastric cancer tissues. *A,* real-time RT-PCR analysis of *LRRC3B* mRNA from 96 primary gastric cancer tissues and adjacent normal tissues. Each value was normalized to the expression of β-*actin*. *LRRC3B* expression was significantly reduced in tumors ($P < 0.0001$). The box plot analysis shows the median, 25th, and 75th percentiles. *B,* pyrosequencing analysis of 6 CpG sites of *LRRC3B* (see Fig. 1*A*) from 78 paired primary gastric tumor tissues and adjacent normal tissues. *LRRC3B* methylation was significantly elevated in tumors compared with normal tissues ($P < 0.0001$). *Points,* mean from 78 samples; *bars,* SD.

[14] http://genome.ucsc.edu/

island. Acetylation levels of histones H3 and H4 at the *LRRC3B* CpG island were elevated in SNU-484 cells in which the *LRRC3B* CpG island is unmethylated and transcriptionally active (Fig. 2*D*). These results clearly indicate that histone deacetylation is also a feasible mechanism for the observed transcriptional silencing of *LRRC3B* in gastric cancer.

***LRRC3B* is frequently silenced and aberrantly methylated in primary gastric cancers.** To examine *LRRC3B* expression during gastric carcinogenesis, we performed real-time RT-PCR in 96 paired gastric tumor and adjacent normal tissues. *LRRC3B* expression was significantly reduced in tumors ($P < 0.0001$; Fig. 3*A*). A majority (88.5%; 85 of 96) of tumors expressed *LRRC3B* at a level lower than

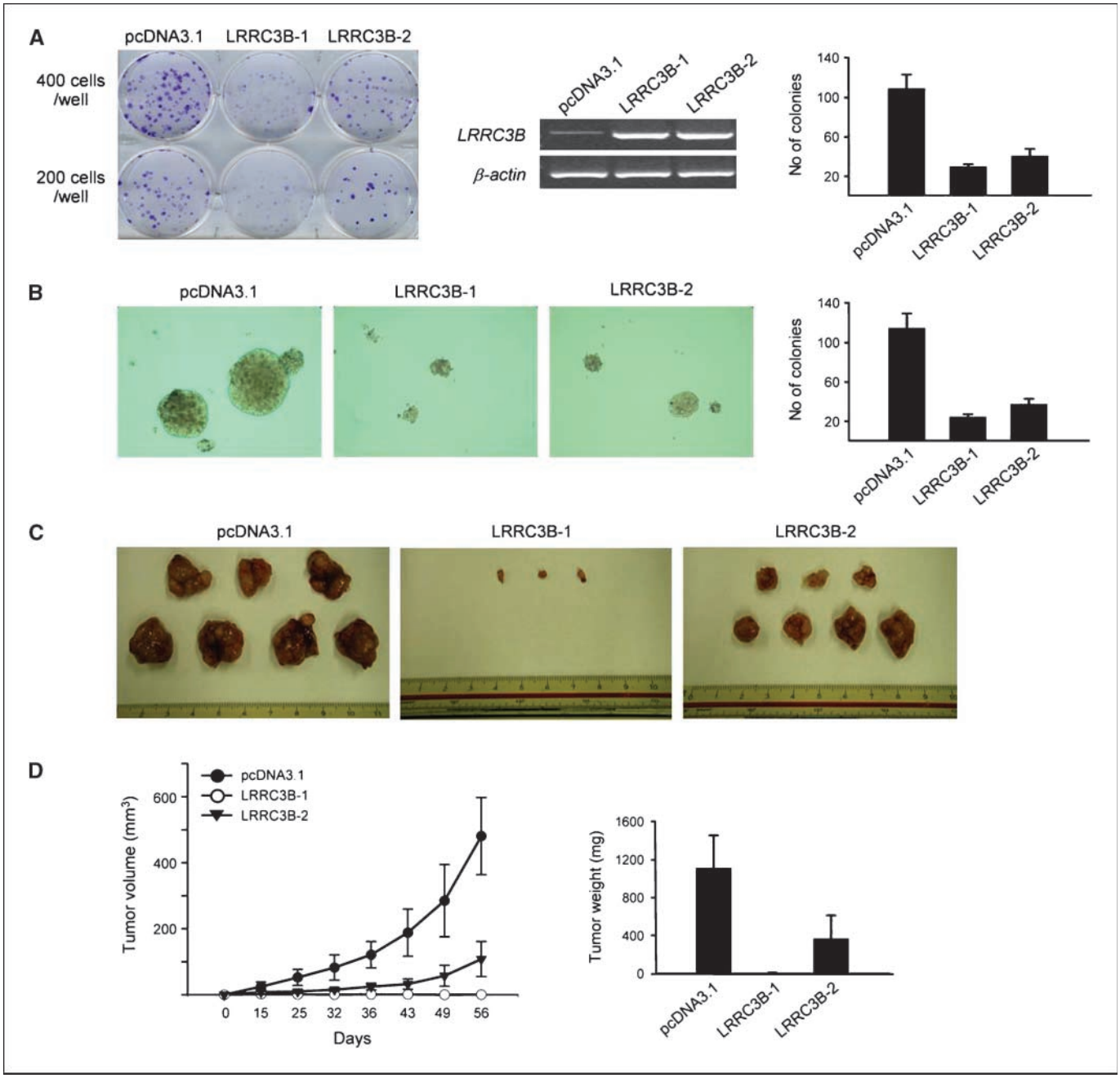

Figure 4. LRRC3B has tumor suppressor activity. *A,* anchorage-dependent colony formation assay in monolayer culture. SNU-601 cells were stably transfected with either pcDNA3.1-LRRC3B or empty vector pcDNA3.1. Two positive clones (LRRC3B-1 and LRRC3B-2) and one control clone (pcDNA3.1) were plated in 6-well plates at 200 or 400 cells per well. After 2 wk of incubation, the cells were stained with crystal violet. RT-PCR analysis of *LRRC3B* mRNA in the three cell lines is shown. The graph shows the number of colonies formed by each stable transfectant. *Columns,* mean of three independent experiments, each performed in duplicate; *bars,* SD. *B,* anchorage-independent colony formation assay in soft agar. The stably transfected cells were plated in top medium with 0.3% agarose over a bottom medium containing 0.6% agarose. Colonies were counted after 2 wk of incubation. The graph shows the number of colonies formed by each stable transfectant. *Columns,* mean of three separate experiments, each performed in duplicate; *bars,* SD. *C,* photographs of tumors excised at 56 d after injection into nude mice of stably transfected cells—two LRRC3B-expressing SNU-601 cell lines and one control vector–transfected SNU-601 cell line. *D,* the left graph shows tumor volume as calculated on the indicated days, and the right graph shows tumor weight at the end of the experiment. *Columns and points,* mean; *bars,* SD.

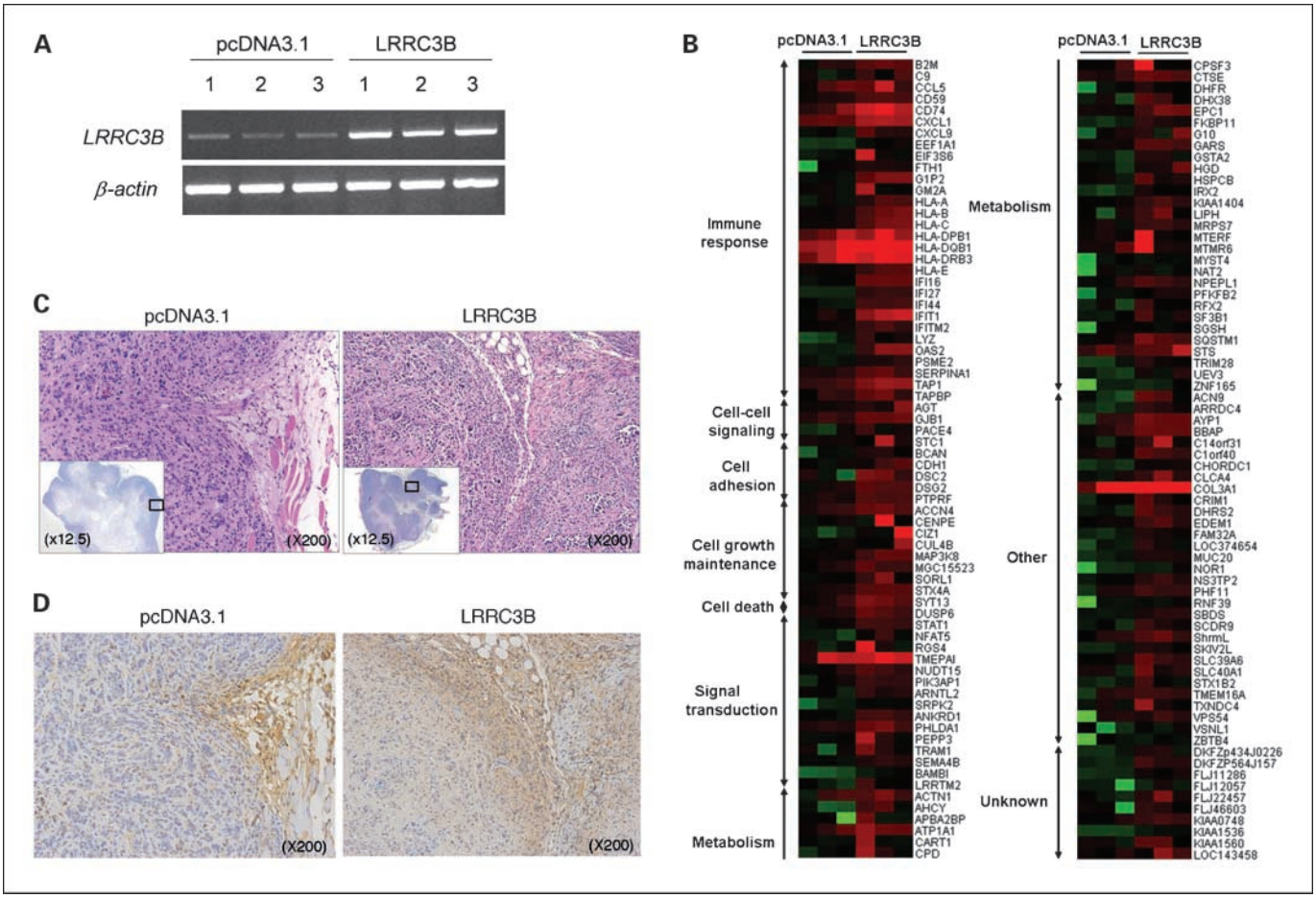

Figure 5. *LRRC3B*-expressing xenograft tumors are sensitized to immune surveillance in nude mice. *A,* RT-PCR analysis of *LRRC3B* mRNA in three pairs of xenograft tumors derived from the LRRC3B-2 stable cell line or control cell line (see Fig. 4*C*). *B,* microarray analysis of gene expression changes in xenograft tumors. Clustering diagram of differentially expressed genes in *LRRC3B*-expressing and control xenograft tumors. One hundred forty genes with a 1.5-fold greater signal in *LRRC3B*-expressing tumors compared with tumors derived from pcDNA3.1-transfected cells were selected. *C,* photographs of xenograft tumors from pcDNA3.1-transfected and *LRRC3B*-expressing cells after H&E staining. *Insets,* show the overall features of the tumor (×12.5) and the black square outlines the magnified region. *D,* infiltration of NK cells in each tumor was visualized by immunostaining for NK cells with an antibody to mouse NK-1.1.

their respective paired normal tissue, and 65.6% (63 of 96) of the tumors showed a >2-fold decrease. Supplementary Table S1 presents clinicopathologic characteristics of patients based on *LRRC3B* expression level. *LRRC3B* down-regulation in tumors was more frequent in tumor-node-metastasis (TNM) stage I than stages II to IV ($P = 0.0351$), suggesting that down-regulation may be an early event in multistep gastric carcinogenesis.

We next performed pyrosequencing to measure the extent of methylation of 6 CpG sites (Fig. 1*A*) in the *LRRC3B* CpG island in 78 paired normal and tumor tissues for which genomic DNA was available. *LRRC3B* methylation was significantly elevated in tumors compared with normal tissue at all CpG sites tested ($P < 0.0001$; Fig. 3*B*). *LRRC3B* methylation in gastric tumor tissues with respect to clinicopathologic characteristics is shown in Supplementary Table S2. Tumors of TNM stage I were methylated more frequently than tumors of stages II to IV ($P = 0.0208$). This methylation status corresponded well to low *LRRC3B* expression in stage I tumors. In addition, intestinal-type tumors were more frequently methylated than diffuse-type tumors ($P = 0.0170$).

LRRC3B is a membrane protein that is highly conserved among vertebrates. *In silico* analysis of the *LRRC3B* open reading frame predicted LRRC3B to be a ~29.3-kDa protein with a signal peptide, an LRR NH_2-terminal domain, three internal LRRs, an LRR COOH-terminal domain, and a transmembrane domain (Supplementary Fig. S1*A*). The GFP-LRRC3B fusion protein localized to the cell membrane, as shown in Supplementary Fig. S1*B*. The amino acid sequence of human LRRC3B is 100% identical to chimpanzee and dog, differs by only one residue from LRRC3B of mouse and rat, and differs by two residues from LRRC3B of cow and pig (Supplementary Fig. S1*C*), indicating that LRRC3B has been highly conserved throughout vertebrate evolution.

LRRC3B has tumor suppressor activity *in vitro* and *in vivo*. To examine the possible activity of LRRC3B as a tumor suppressor, we performed colony formation assay and tumorigenesis assay. We established stably transfected LRRC3B-expressing SNU-601 cell lines. Among the gastric cancer cell lines in which *LRRC3B* is hypermethylated and transcriptionally silenced, our previous experiments established that SNU-601 cells are the most proficient at forming tumors in nude mice. SNU-216 cells also form tumors, but SNU-638 seldom do so in nude mice. Two independent stably transfected LRRC3B-expressing SNU-601 cell lines (LRRC3B-1 and LRRC3B-2) formed fewer colonies than the empty vector–transfected cells in the anchorage-dependent assay (Fig. 4*A*). Moreover, the LRRC3B-1 and LRRC3B-2 transfectants

also formed fewer colonies than the control cells in an anchorage-independent assay on soft agar (Fig. 4*B*). These results suggest that LRRC3B suppresses cell proliferation signals in gastric cancer cells. We next examined the effect of LRRC3B overexpression by a tumorigenesis assay in nude mice. Nude mice were injected with the two stably transfected LRRC3B-expressing SNU-601 cell lines or empty vector–transfected cells, sacrificed 8 weeks after injection, and their tumors were dissected and weighed (Fig. 4*C*). The control cells formed rapidly growing tumors, whereas the LRRC3B-1 and LRRC3B-2 cells formed tumors that were much smaller (Fig. 4*D*), suggesting that LRRC3B has tumor suppressor activity and is a negative regulator of tumor growth both *in vitro* and *in vivo*.

Tumorigenicity of LRRC3B-transfected cells in nude mice is inhibited by immune responses. To understand how LRRC3B exerted tumor suppressor activity in xenografted mice, we compared the gene expression profiles of tumors derived from LRRC3B-2 cells and control vector–transfected cells using cDNA microarrays. We initially planned a transcriptome analysis using a microarray for the xenograft tumors derived from the LRRC3B-1 line as well as the LRRC3B-2 line; however, the tumors derived from LRRC3B-1 cell were too small to obtain enough RNA to be used in a microarray analysis. *LRRC3B* mRNA expression level in three xenograft tumors derived from LRRC3B-2 cells and three control tumors was confirmed by RT-PCR (Fig. 5*A*). We identified 140 genes with a >1.5-fold increase in expression in *LRRC3B*-expressing xenograft tumors and categorized those selected genes into functional groups (Fig. 5*B*). Seven categories potentially linked to the inhibition of tumor growth were identified, including mediators of immune responses, cell-cell signaling, cell adhesion, cell growth, cell death, signal transduction, and metabolism. Remarkably, 30 genes potentially promoting the immune responses showed increased expression in the *LRRC3B*-expressing xenograft tumors, and 11 genes among them were related to IFN response (Supplementary Table S3).

In H&E-stained sections, the *LRRC3B*-expressing xenograft tumor showed several lobular tumors and infiltrating lymphocytes, whereas the control cell–derived xenograft tumor showed a nonlobular form and few infiltrating lymphocytes (Fig. 5*C*). The presence of lymphocytes in the *LRRC3B*-expressing xenograft tumor was much more pronounced around each lobule. Compared with wild-type mice, athymic nude mice have higher levels of natural killer (NK) cells and fewer T cells that can contribute to immune surveillance (34, 35). To determine the infiltration of NK cells in each xenograft tumor, we visualized NK cells by immunostaining. A strong infiltration of positively stained NK cells was observed only in the *LRRC3B*-expressing tumors, whereas little or no infiltration of NK cell marker–positive cells was observed within control cell–derived xenograft tumors (Fig. 5*D*), indicating that the *LRRC3B*-expressing xenograft tumor was sensitized to lymphocytes such as NK cells. These results suggest that the *LRRC3B*-expressing xenograft tumor was sensitized to immune surveillance in nude mice.

Discussion

Our results show that *LRRC3B* expression is repressed in gastric cancer cells by epigenetic mechanisms and that its normal expression results tumor suppressor activity both *in vitro* and *in vivo*, suggesting that it is a new tumor suppressor gene in gastric cancer, as based on several lines of evidence. First, expression of *LRRC3B* was repressed in most of the gastric cancer cell lines (90.9%) and gastric tumor tissues (88.5%) we tested. Second, the chromosome 3p region, where human *LRRC3B* (3p24.1) is located, is one of the most frequently deleted chromosomal regions in gastric cancers (36, 37). For example, *RASSF1A*, at chromosome 3p21.3, is a tumor suppressor gene frequently silenced in gastric cancers by epigenetic modification and loss of heterozygosity (38). Third, restoration of *LRRC3B* expression in gastric cell lines strongly inhibited cell growth both in anchorage-dependent and anchorage-independent assays. Finally, expression of *LRRC3B* in xenografted mice greatly reduced tumor growth.

Epigenetic modification was the main mechanism of *LRRC3B* inactivation in the gastric cancer specimens we tested, with *LRRC3B* expression silenced by promoter hypermethylation. Sixty-seven percent of the primary gastric tumors showed >2-fold decreased expression levels of *LRRC3B*, and most of them had hypermethylated CpG sites in the *LRRC3B* promoter region. We also investigated the possibility of genetic mutations inactivating *LRRC3B* but found no nonsynonymous or frameshift mutations in the *LRRC3B* coding region (data not shown). Acetylation levels of histone H3 and H4 at the *LRRC3B* CpG island were decreased in the gastric cancer cell lines we tested, in which the *LRRC3B* CpG island is hypermethylated and transcriptionally silenced. Thus, DNA hypermethylation and histone deacetylation seem to be the main mechanisms of inactivation of *LRRC3B* in gastric cancer. Among subtypes of gastric tumors, *LRRC3B* expression was more frequently reduced in early-stage gastric cancer than in advanced-stage gastric cancer. Although epigenetic silencing of genes can occur at any time during tumor progression, it occurs most frequently during early stages (14, 39). The frequent loss of *LRRC3B* expression in early-stage gastric cancer suggests that epigenetic silencing of *LRRC3B* is an important event in tumor initiation.

To understand how LRRC3B exerts its tumor suppressive function, we performed microarray analysis with xenograft tumors derived from a stable *LRRC3B*-expressing cell line, as gene expression analysis of xenograft models can give useful information about *in vivo* tumorigenesis mechanisms involving secreted and cell surface proteins (40, 41). Our microarray analysis showed that the most significant gene expression change in the *LRRC3B*-expressing xenograft tumors was the induction of genes involved in the immune response and IFN pathways. CD59, CD74, and MHC class I antigens are important in recognition by the immune system. Down-regulation of MHC class I antigens and loss of tumor antigens is a major mechanism by which tumor cells escape immune surveillance (42). The induction of immune recognition genes in *LRRC3B*-expressing xenograft tumors suggests that one of the tumor suppressive mechanisms of LRRC3B is the induction of immune recognition against tumors and lymphocyte infiltration. In fact, we found many infiltrating lymphocytes in H&E-stained sections of an *LRRC3B*-expressing xenograft tumor. IFN pathway genes were also induced. The IFN signaling pathway is growth suppressive, and multiple IFN pathway genes are epigenetically silenced after cellular immortalization (43). Also, some IFN signaling genes such as *RNaseL* (44) and *IRF-1* (45) show tumor suppressor activity. Additionally, the well-established tumor suppressor genes *BRCA1* and *DAP kinase* have been identified as components in the IFN γ–regulated signaling pathway (46).

In summary, inactivation of *LRRC3B*, which encodes a membrane protein, may be a critical event in the early stages of gastric cancer tumorigenesis that induces cancer cells to escape immune

surveillance. We suggest that *LRRC3B* is a tumor suppressor gene that triggers the innate immune response by lymphocyte infiltration and activation of the IFN signaling pathway.

Disclosure of Potential Conflicts of Interest

No potential conflicts of interest were disclosed.

Acknowledgments

Received 2/22/2008; revised 5/2/2008; accepted 5/14/2008.

Grant support: FG08-11-01 of the 21C Frontier Functional Human Genome Project from the Ministry of Science and Technology of Korea.

The costs of publication of this article were defrayed in part by the payment of page charges. This article must therefore be hereby marked *advertisement* in accordance with 18 U.S.C. Section 1734 solely to indicate this fact.

References

1. Clark HF, Gurney AL, Abaya E, et al. The secreted protein discovery initiative (SPDI), a large-scale effort to identify novel human secreted and transmembrane proteins: a bioinformatics assessment. Genome Res 2003;13:2265–70.
2. Kobe B, Deisenhofer J. A structural basis of the interactions between leucine-rich repeats and protein ligands. Nature 1995;374:183–6.
3. Kajava AV, Kobe B. Assessment of the ability to model proteins with leucine-rich repeats in light of the latest structural information. Protein Sci 2002;11:1082–90.
4. Kobe B, Kajava AV. The leucine-rich repeat as a protein recognition motif. Curr Opin Struct Biol 2001;11:725–32.
5. Kajava AV. Structural diversity of leucine-rich repeat proteins. J Mol Biol 1998;277:519–27.
6. Pancer Z, Cooper MD. The evolution of adaptive immunity. Annu Rev Immunol 2006;24:497–518.
7. Chen X, Leung SY, Yuen ST, et al. Variation in gene expression patterns in human gastric cancers. Mol Biol Cell 2003;14:3208–15.
8. Richardson AL, Wang ZC, De Nicolo A, et al. X chromosomal abnormalities in basal-like human breast cancer. Cancer Cell 2006;9:121–32.
9. Bianchini M, Levy E, Zucchini C, et al. Comparative study of gene expression by cDNA microarray in human colorectal cancer tissues and normal mucosa. Int J Oncol 2006;29:83–94.
10. Korkola JE, Houldsworth J, Chadalavada RS, et al. Down-regulation of stem cell genes, including those in a 200-kb gene cluster at 12p13.31, is associated with *in vivo* differentiation of human male germ cell tumors. Cancer Res 2006;66:820–7.
11. Lapointe J, Li C, Higgins JP, et al. Gene expression profiling identifies clinically relevant subtypes of prostate cancer. Proc Natl Acad Sci U S A 2004;101:811–6.
12. Sun L, Hui AM, Su Q, et al. Neuronal and glioma-derived stem cell factor induces angiogenesis within the brain. Cancer Cell 2006;9:287–300.
13. Herman JG, Baylin SB. Gene silencing in cancer in association with promoter hypermethylation. N Engl J Med 2003;349:2042–54.
14. Baylin SB, Ohm JE. Epigenetic gene silencing in cancer - a mechanism for early oncogenic pathway addiction? Nat Rev Cancer 2006;6:107–16.
15. Laird PW. The power and the promise of DNA methylation markers. Nat Rev Cancer 2003;3:253–66.
16. Kim JH, Lee KT, Kim HC, et al. Cloning of NotI-linked DNA detected by restriction landmark genomic scanning of human genome. Genomics & Informatics 2006;4:1–10.
17. Kim SK, Jang HR, Kim JH, et al. The epigenetic silencing of LIMS2 in gastric cancer and its inhibitory effect on cell migration. Biochem Biophys Res Commun 2006;349:1032–40.
18. Kim M, Lee KT, Jang HR, et al. Epigenetic down-regulation and suppressive role of DCBLD2 in gastric cancer cell proliferation and invasion. Mol Cancer Res 2008;6:222–30.
19. Kim M, Jang HR, Kim JH, et al. Epigenetic inactivation of Protein Kinase D1 in gastric cancer and its role in gastric cancer cell migration and invasion. Carcinogenesis 2008;29:629–37.
20. Park JG, Frucht H, LaRocca RV, et al. Characteristics of cell lines established from human gastric carcinoma. Cancer Res 1990;50:2773–80.
21. Park JG, Yang HK, Kim WH, et al. Establishment and characterization of human gastric carcinoma cell lines. Int J Cancer 1997;70:443–9.
22. Hatada I, Hayashizaki Y, Hirotsune S, Komatsubara H, Mukai T. A genomic scanning method for higher organisms using restriction sites as landmarks. Proc Natl Acad Sci U S A 1991;88:9523–7.
23. Nagai H, Tsumura H, Ponglikitmongkol M, Kim YS, Matsubara K. Genomic aberrations in human hepatoblastomas detected by 2-dimensional gel analysis. Cancer Res 1995;55:4549–51.
24. Nagai H, Pongliktmongkol M, Kim YS, Yoshikawa H, Matsubara K. Cloning of NotI-cleaved genomic DNA fragments appearing as spots in 2D gel electrophoresis. Biochem Biophys Res Commun 1995;213:258–65.
25. Nagai H, Ponglikitmongkol M, Mita E, et al. Aberration of genomic DNA in association with human hepatocellular carcinomas detected by 2-dimensional gel analysis. Cancer Res 1994;54:1545–50.
26. Johnson MR, Wang K, Smith JB, Heslin MJ, Diasio RB. Quantitation of dihydropyrimidine dehydrogenase expression by real-time reverse transcription polymerase chain reaction. Anal Biochem 2000;278:175–84.
27. Han DC, Lee MY, Shin KD, et al. 2′-benzoyloxycinnamaldehyde induces apoptosis in human carcinoma via reactive oxygen species. J Biol Chem 2004;279:6911–20.
28. Kim SY, Kim JH, Lee HS, et al. Meta- and gene set analysis of stomach cancer gene expression data. Mol Cells 2007;24:200–9.
29. Tusher VG, Tibshirani R, Chu G. Significance analysis of microarrays applied to the ionizing radiation response. Proc Natl Acad Sci U S A 2001;98:5116–21.
30. Kim JM, Sohn HY, Yoon SY, et al. Identification of gastric cancer-related genes using a cDNA microarray containing novel expressed sequence tags expressed in gastric cancer cells. Clin Cancer Res 2005;11:473–82.
31. Esteller M. Cancer epigenomics: DNA methylomes and histone-modification maps. Nat Rev Genet 2007;8:286–98.
32. Jones PA, Taylor SM. Cellular differentiation, cytidine analogs and DNA methylation. Cell 1980;20:85–93.
33. Yoshida M, Kijima M, Akita M, Beppu T. Potent and specific inhibition of mammalian histone deacetylase both *in vivo* and *in vitro* by trichostatin A. J Biol Chem 1990;265:17174–9.
34. Kim R, Emi M, Tanabe K. Cancer immunoediting from immune surveillance to immune escape. Immunology 2007;121:1–14.
35. Maleckar JR, Sherman LA. The composition of the T cell receptor repertoire in nude mice. J Immunol 1987;138:3873–6.
36. Yustein AS, Harper JC, Petroni GR, Cummings OW, Moskaluk CA, Powell SM. Allelotype of gastric adenocarcinoma. Cancer Res 1999;59:1437–41.
37. Choi SW, Park SW, Lee KY, Kim KM, Chung YJ, Rhyu MG. Fractional allelic loss in gastric carcinoma correlates with growth patterns. Oncogene 1998;17:2655–9.
38. Dammann R, Li C, Yoon JH, Chin PL, Bates S, Pfeifer GP. Epigenetic inactivation of a RAS association domain family protein from the lung tumour suppressor locus 3p21.3. Nat Genet 2000;25:315–9.
39. Feinberg AP, Tycko B. The history of cancer epigenetics. Nat Rev Cancer 2004;4:143–53.
40. Stull RA, Tavassoli R, Kennedy S, et al. Expression analysis of secreted and cell surface genes of five transformed human cell lines and derivative xenograft tumors. BMC Genomics 2005;6:55.
41. Creighton C, Kuick R, Misek DE, et al. Profiling of pathway-specific changes in gene expression following growth of human cancer cell lines transplanted into mice. Genome Biol 2003;4:R46.
42. Khong HT, Restifo NP. Natural selection of tumor variants in the generation of "tumor escape" phenotypes. Nat Immunol 2002;3:999–1005.
43. Kulaeva OI, Draghici S, Tang L, Kraniak JM, Land SJ, Tainsky MA. Epigenetic silencing of multiple interferon pathway genes after cellular immortalization. Oncogene 2003;22:4118–27.
44. Carpten J, Nupponen N, Isaacs S, et al. Germline mutations in the ribonuclease L gene in families showing linkage with HPC1. Nat Genet 2002;30:181–4.
45. Harada H, Kitagawa M, Tanaka N, et al. Anti-oncogenic and oncogenic potentials of interferon regulatory factors-1 and -2. Science 1993;259:971–4.
46. Andrews HN, Mullan PB, McWilliams S, et al. BRCA1 regulates the interferon γ-mediated apoptotic response. J Biol Chem 2002;277:26225–32.

LRRC3B, Encoding a Leucine-Rich Repeat-Containing Protein, Is a Putative Tumor Suppressor Gene in Gastric Cancer

Mirang Kim, Jeong-Hwan Kim, Hay-Ran Jang, et al.

Cancer Res 2008;68:7147-7155.